Science of the Total Environment 869 (2023) 161831

Contents lists available at ScienceDirect

Science of the Total Environment

journal homepage: www.elsevier.com/locate/scitotenv

Critical fire weather conditions during active fire spread days in Canada

Xianli Wang [a,*], Jacqueline Oliver [b], Tom Swystun [c], Chelene C. Hanes [c], Sandy Erni [c], Mike D. Flannigan [b]

[a] Northern Forestry Centre, Canadian Forest Service, Natural Resources Canada, 5320-122nd Street, Edmonton, AB T6H 3S5, Canada
[b] Dept of Natural Resource Science, Faculty of Science, Thompson Rivers University, 805 TRU Way, Kamloops, BC V2C 0C8, Canada
[c] Great Lakes Forestry Centre, Canadian Forest Service, Natural Resources Canada, 1219 Queen Street East, Sault Ste. Marie, ON P6A 2E5, Canada

HIGHLIGHTS

- A spread day occurs under less severe fire weather conditions with the increase of latitude.
- FFMC is mostly consistent across all spatial scales during a spread day.
- FFMC, ISI, and FWI are the best for spread day identification and prediction.

GRAPHICAL ABSTRACT

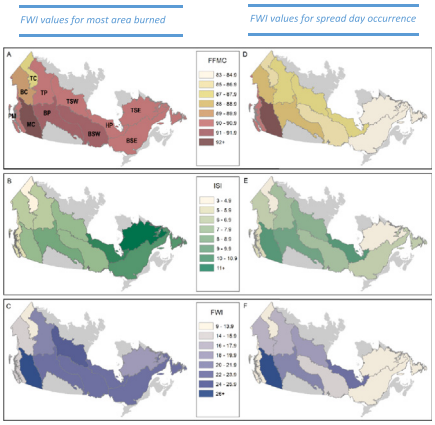

ARTICLE INFO

Editor: Manuel Esteban Lucas-Borja

Keywords:
Fire weather
Spread day
Thresholds
Area burned
Canada

ABSTRACT

A spread day is defined as a day in which fires grow a substantial amount of area; such days usually occur during high or extreme fire weather conditions. The identification and prediction of a spread day based on fire weather conditions could help both our understanding of fire regimes as well as forecasting and managing fires operationally. This study explores the relationships between fire weather and spread days in the forested areas of Canada by spatially and temporally matching a daily fire growth database to a daily gridded fire weather database that spans from 2001 to 2019. By examining the correlations between spread day fire weather conditions and location, conifer coverage (%), and elevation, we found that a spread day happens under less severe fire weather conditions as latitude increases for the entire study area and as conifer coverage increases within non-mountainous study areas. In the western mountain areas, however, with increasing conifer coverage more severe fire weather conditions are required for a spread day to occur. Using two modeling approaches, we were able to identify spread day indicators (generalized additive model) and to predict the occurrence of spread days (semi-binomial regression model) by Canadian Ecozones both annually and seasonally. Overall, Fine Fuel Moisture Code (FFMC), Initial Spread Index (ISI), and Fire Weather Index (FWI) performed the best in all models built for spread day identification and prediction but varied depending on the conditions mentioned above. FFMC was the most consistent across all spatial and temporal scales.

1. Introduction

A large fire may burn for a significant duration until it encounters a substantial rain event, a fuel break, or a change of season (i.e., fire conducive weather) (e.g., spring to summer or winter) limits its growth and allows

* Corresponding author.
E-mail address: xianli.wang@nrcan-rncan.gc.ca (X. Wang).

http://dx.doi.org/10.1016/j.scitotenv.2023.161831
Received 28 November 2022; Received in revised form 21 January 2023; Accepted 21 January 2023
Available online 25 January 2023

for its containment or extinguishment (Latham and Rothermel, 1993). Despite their relative longevity, fires burn most of their area during just a few days of high or extreme fire weather (Rothermel et al., 1994) referred to as "spread days" (Podur and Wotton, 2011). Fire conducive weather is necessary for active fire growth, and a spread day is the realization of the fire weather potential (Wang et al., 2014). Thresholds used to determine "high or extreme fire weather" that may lead to a realized spread day are therefore crucial to fire management. Every province in Canada has a fire danger rating chart based on fire weather conditions that are widely used by the fire management agency as well as the public (see Hanes et al., 2022), and fire research (e.g., Wang et al., 2017a, 2022; Richardson et al., 2021; Coop et al., 2022). For example, a fire weather index (FWI; Van Wagner, 1987) ≥ 19 has commonly been used to identify a spread day (e.g., Parisien et al., 2013; Wang et al., 2015, 2017a, 2022; Zong et al., 2021); however, this threshold was estimated based on data from eastern Canada (Podur and Wotton, 2011), and may be biased as fire conducive weather conditions change with fuel type and environmental conditions (e.g., Forestry Canada Fire Danger Group, 1992). Therefore, a more thorough and systematic exploration of regional critical fire weather conditions across the entire forested region of the country is needed. Such an exploration is now possible due to the development of historical fire growth mapping techniques (Parks, 2014) and coast-to-coast, historical daily fire weather data (McElhinny et al., 2020).

The two types of data needed to explore the relationship between fire weather condition and fire growth include 1) the delineation of daily fire growth and 2) the weather conditions associated with it. Historically, weather data are primarily obtained from weather stations but due to the scarcity of weather stations in northern Canada (e.g., Hanes et al., 2017; Cai et al., 2019) it can be difficult to ensure that the weather station data is representative of an ongoing fire. This issue has been addressed with the completion of the global gridded fire weather database (McElhinny et al., 2020). Daily fire growth delineation has typically been accomplished using remote sensing products (e.g., Valero et al., 2017, 2018; Oliver et al., 2022); however, because of the lack of high-resolution data and the concealment of fire activity on the ground by smoke and clouds, fire growth mapping must be supplemented by modeling techniques (e.g., Parks, 2014). These modeling techniques take advantage of both the more accurate fire perimeters (e.g., Hall et al., 2020) and new remote sensing products (Moderate Resolution Imaging Spectroradiometer (MODIS) and Visible Infrared Imaging Radiometer Suite (VIIRS)) to map the daily growth of historical fires at a continental scale (e.g., Wang et al., 2014, 2022) or even broader. The relationships between fire weather conditions and spread days can therefore be examined.

In Canada, the Canadian Forest Fire Weather Index (FWI) System (Van Wagner, 1987) has been used to assess relative fire danger. Because these indices were designed to reflect the highest fire-conducive weather conditions of a given day, determining the values or thresholds mostly commonly associated with spread days would be beneficial for both fire management and fire research activity (see also Podur and Wotton, 2011; Hanes et al., 2022). The FWI System contains six indices to characterize potential fuel moisture and fire behavior (Van Wagner, 1987): the Fine Fuel Moisture Code (FFMC), the Duff Moisture Code (DMC), and the Drought Code (DC) track moisture in different ground fuel layers, while the Initial Spread Index (ISI), the Build-up Index (BUI), and the Fire Weather Index (FWI) assess potential fire spread, fuel availability, and fire intensity, respectively. A larger FWI System moisture code indicates drier conditions, and a larger index unit represents the potential for more extreme fire behavior, due to more severe underlying fire weather conditions. However, FFMC, ISI, and FWI are more widely used than the others for the identification of spread days (British Columbia and Alaska use BUI instead e.g., Wang et al., 2016, 2020; Barber et al., 2018; Stralberg et al., 2018) because they change with the variation of weather conditions at a finer temporal scale (Van Wagner, 1977).

The linkage between fire weather potential (i.e., number of spread days) and fire growth has been established using complicated statistical models (e.g., Wang et al., 2020; Abatzoglou et al., 2021; Coop et al., 2022). However, using thresholds to define a weather-based spread day has never been thoroughly examined and quantified considering the spatial and temporal (i.e., seasonal) heterogeneity of the country. Analysis by Podur and Wotton (2011) focused only on the province of Ontario, which encompasses parts of the boreal shield east and west and the Hudson plains. The use of universal FWI System index thresholds to identify a spread day over a large area may become problematic for regional fire management (see Hanes et al., 2022) and fire hazard assessment (e.g., Parisien et al., 2013; Wang et al., 2016), although from a pure simulation modeling perspective this may not be critical (e.g., Wang et al., 2017a, 2022). In addition, the availability of gridded fire weather data now presents the opportunity to better quantify the spatial and temporal variations of fire-weather conditions for spread days. The objectives in this study are therefore to (1) examine the thresholds of the FWI System indices for a spread day across Canada; (2) model the occurrence of spread days based on FWI System indices; (3) explore factors affecting the spatial and temporal variations of the spread day fire weather conditions.

2. Method

2.1. Study area

Our study area is the forested landmass of Canada, excluding all islands in both the Pacific and Atlantic Oceans. The Rocky Mountain range in Canada extends from western Alberta westward to British Columbia, northward into the Yukon, and includes parts of the Northwest Territories. The remainder of the country, to the east of the Rocky Mountains and extending to the Atlantic Ocean, accounts for the majority of the study area and is relatively flat (non-mountainous). The forested area of Canada is represented by three major biomes including the boreal forests that extend across central Canada and to the southern edge of the Tundra, the temperate coniferous forests on the west coast, and the temperate broadleaf and mixed forests that predominate the east coast and Great Lakes area. We used the Canadian Ecozones (ESWG, 1996) as the primary analysis unit but, following Stocks et al. (2002) (Fig. 1A), we split the Taiga Shield and Boreal Shield Ecozones into west and east components due to climate and fire activity disparities. We also used the finer scale fire regime units (FRU; Erni et al., 2020; Fig. 1B) to examine variations in spread day thresholds in accordance with elevation, temperature, and conifer coverage gradient across the country.

2.2. Data

2.2.1. Fire data

The National Burned Area Composite (NBAC) dataset (Hall et al., 2020) was used in this study; it is a GIS fire polygon database derived from 30-m Landsat imagery and high-quality agency imagery with a spatial resolution <30 m that includes fires that occurred between 1986 and 2019. The NBAC is considered the most consistent and accurate wildfire polygon database in Canada for that time (Hanes et al., 2019). Fires >50 ha (e.g., Wang et al., 2021) between 2001 and 2019 (5190 fires in total) were used in the study in accordance with the availability of MODIS and VIIRS products.

2.2.2. Fire weather data

A subset of the Global Fire Weather Indices dataset (McElhinny et al., 2020) was used in this study. These 0.25° resolution gridded FWI System indices were calculated using the European Centre for Medium-range Weather Forecasts (ECMWF) ERA5-HRS Reanalysis product (C3S, 2017) as inputs to functions in the cffdrs R Package (Wang et al., 2017b). The consideration of overwintering DC in the calculation of the FWI System indices make this database state of the art, based on currently available models and inputs, with complete coverage of our study area. The authors of the database have updated its coverage to include the year of 2019, which makes it possible for us to include these fires (McElhinny et al., 2020).

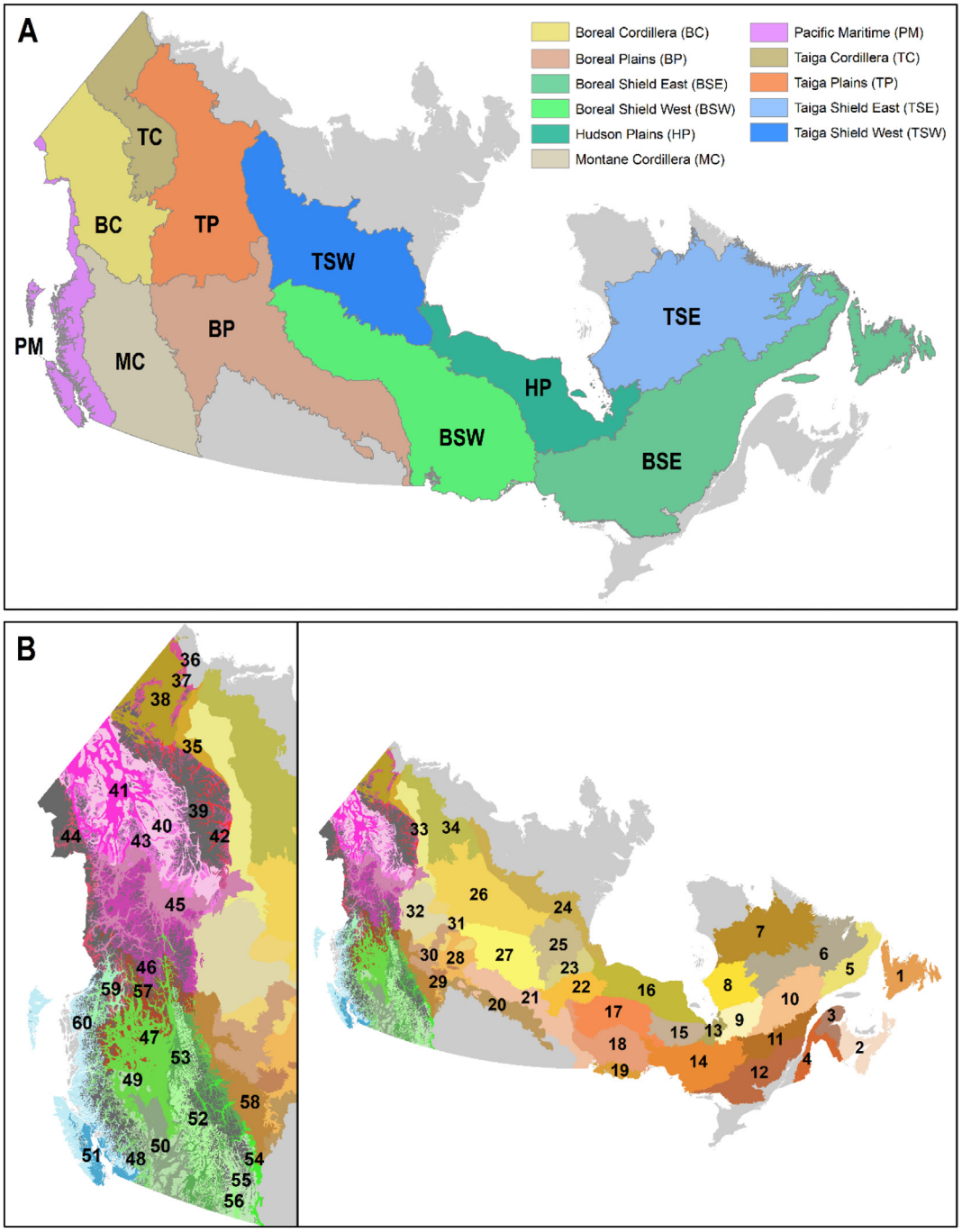

Fig. 1. A. The Canadian Ecozones (ESWG, 1996). Southern Arctic, Mixed Wood Plains, and Atlantic Maritime were excluded from the study due to insufficient fire data. B. Fire regime units (FRUs), where the left panel is the mountainous region and the right panel is the non-mountainous region.

2.2.3. Mapping daily fire growth

In this study, a fire growth mapping technique developed by Parks (2014) was used to delineate daily fire growth. Because MODIS[1] data is available since 2001 and VIIRS[1] data since 2013, we mapped daily fire spread using the NBAC fire perimeters (≥ 50 ha) and MODIS hotspots for fires that occurred from 2001 to 2012 and used MODIS hotspots and VIIRS hotspots for fires that occurred from 2013 to 2019. Daily fire growth was mapped at a 30-m resolution by spatially interpolating the 1-km (MODIS) or 375 m (VIIRS) resolution remote sensing hotspots, and the NBAC fire polygons were used to constrain the final fire size of the interpolation (Parks, 2014). A spread day was determined to have occurred when daily fire growth, calculated for a nominal rate of spread of at least 1 m min^{-1}, had surpassed a spread distance of 240 m following a circular growth model assuming 4 h of active burning per day (c.f., Hirsch, 1996; Wang et al., 2014, 2022).

By identifying the nearest ERA5-based fire weather grid points to the daily burned area (multiple points were included when fires were very large), we paired daily fire growth with the daily fire weather condition (local noon) for all fires considered in the study from 2001 to 2019. Therefore, most of our analysis in this study was conducted based on the dataset we assembled, except for the FRU-based mean elevation, latitude (centroid), and conifer coverage that were extracted separately.

[1] NASA MCD14ML product, Collection 5, Version 1, available at: https://fsapps.nwcg.gov/afm/activefiremaps.php

2.3. Analysis

Because the cause(s) of a given spread day are not always the same, it was necessary to analyze the entire suite of fire weather indices (Van Wagner, 1987).

2.3.1. Summary stats

We compared the difference (*t*-test) between the fire weather conditions that occurred during spread days and non-spread days. If a significant difference ($\alpha = 0.05$) was present between the two groups, it validated the use of fire weather variables to differentiate between spread and non-spread days. The correlation test was performed on the entire study area, as well as on subsets determined by Ecozone, to detect trends between SD thresholds and environmental variables. Based on the spread day fire weather conditions at the FRU level, we also examined the relationships (Pearson's correlation coefficient) between the mean FWI System indices for spread days and latitude (unit centroid), elevation (mean), and conifer coverage (%).Following Wang et al. (2021), we also conducted the same correlation test for the mountain area (FRU units 35 and above) and non-mountainous area (FRU units 35 and below; Fig. 1B).

2.3.2. Fire weather conditions that support the most area burned

We summarized the total area burned by unit FWI System indices based on the paired daily fire growth and daily fire weather condition data we assembled. For example, area burned for FFMC = 90 is a summation of all the areas burned with FWI between 89.5 and 90.5. Area burned (%) was then calculated for each unit FWI system index as a proportion of the total area burned for all spread days at all units. A generalized additive model (GAM; Hastie and Tibshirani, 1990) was fit between area burned (%) and the FWI System indices. The `gam` function from the R package `mgcv` (Wood, 2011) was used in the analysis. Using these GAMs, we identified the FWI System index values at which the highest area burned for the whole study area, as well as by Ecozone. These values can then be considered the identifiers for the occurrence of a spread day. These examinations were also performed by season (i.e., spring (Mar, Apr, and May), summer (Jun, Jul, and Aug), and fall (Sep, Oct, and Nov)) within each analysis unit. To show the range of those extreme values, we also identified the ranges for the top 5 % area burned cases as most of the area burned is unimodal but non-symmetrically distributed along the FWI System indices gradients. This analysis was beneficial because it allowed us to identify FWI System index values that correspond to spread days without having to rigidly pre-define a spread day.

2.3.3. Modeling the probability of spread day occurrence

To model the probability of spread day occurrence, a pre-defined spread day (i.e., nominal rate of spread >1 m min^{-1} with spread distance >240 m) is needed. By calculating the frequency of spread days (i.e., SD/(SD + NSD), where SD = number of spread days, NSD = number of non-spread days) for each unit FWI System index, we were able to fit a logistic regression model to determine the probability of a spread day occurring for each FWI System index. From these models, we identified the FWI System indices thresholds that correspond to a 50 % chance of a spread day occurring (see also Podur and Wotton, 2011). To improve the model fits, we considered polynomial terms in the model (i.e., quasi-binomial regression model; the exponent goes up to 2, but not any higher

Table 1
Mean FWI indices values (standard deviation) that are not significantly different ($\alpha = 0.05$) between spread days (SD) and non-spread days (Non-SD) by Canadian Ecozone.

Ecozone	Season	Indices	Non-SD	SD	*p*-value
PM	All year	DC	247.7 (80.1)	258.7 (99.1)	0.101
TP	All year	DC	370.6 (135.4)	372.2 (158.0)	0.306
BC	Spring	DMC	36.4 (21.0)	38.7 (18.4)	0.107
BSE	Spring	DMC	39.1 (22.1)	40.8 (17.8)	0.460
TP	Spring	DMC	57.7 (30.2)	59.7 (24.1)	0.388
BC	Spring	DC	122.5 (70.9)	117.3 (71.3)	0.318
BSE	Spring	DC	90.1 (42.9)	85.1 (30.3)	0.266
TC	Spring	DC	53.4 (15.4)	59.2 (17.5)	0.056
TP	Spring	DC	178.6 (94.8)	176.8 (91.6)	0.816
BC	Spring	BUI	41.2 (23.2)	42.6 (20.8)	0.392
BSE	Spring	BUI	40.4 (21.7)	41.3 (17.4)	0.676
TP	Spring	BUI	63.5 (31.3)	65.5 (26.7)	0.429
BP	Fall	DC	426.7 (128.7)	405.2 (93.1)	0.092
BSW	Fall	DC	341.6 (66.6)	341.6 (82.0)	0.986
MC	Fall	DC	489.6 (141.4)	492.1 (149.4)	0.707
TP	Fall	DC	505.2 (110.9)	502.5 (129)	0.688

Table 2
Significant correlations ($\alpha = 0.05$) between mean FWI System variables for spread days and latitude (Lat), elevation (ELV), and conifer coverage (C) at the FRU level over the whole study area.

Fact	Indices	Season	r	p-value
C	BUI	All year	0.26	0.048
C	DC	All year	0.295	0.025
C	DC	Spring	−0.326	0.035
C	FFMC	Summer	0.319	0.015
ELV	BUI	All year	0.385	0.003
ELV	BUI	Fall	0.51	0.002
ELV	BUI	Spring	−0.308	0.047
ELV	BUI	Summer	0.349	0.007
ELV	DC	All year	0.352	0.007
ELV	DC	Fall	0.396	0.017
ELV	DC	Summer	0.281	0.033
ELV	DMC	All year	0.368	0.004
ELV	DMC	Fall	0.521	0.001
ELV	DMC	Spring	−0.334	0.031
ELV	DMC	Summer	0.341	0.009
ELV	FFMC	Summer	0.267	0.043
ELV	FWI	Fall	0.486	0.003
ELV	FWI	Spring	−0.435	0.004
ELV	ISI	Fall	0.362	0.03
ELV	ISI	Spring	−0.434	0.004
Lat	FFMC	All year	−0.328	0.012
Lat	FWI	All year	−0.339	0.009
Lat	FWI	Summer	−0.33	0.011
Lat	ISI	All year	−0.445	0
Lat	ISI	Spring	−0.431	0.004
Lat	ISI	Summer	−0.441	0.001

Table 3
FWI System variable values at which the most area burned (Max) determined based on the GAMs for the whole study area. We also report mean (min, max) FWI System variable values of the top 5 % (top5pc) most area burned cases.

Season	Indices	Sample size	r^2_{adj}	top5pc	Max
All year	BUI	299	0.956	59.8 (51, 68.6)	59.8
Fall	BUI	249	0.770	54.8 (47.3, 62.3)	54.9
Spring	BUI	154	0.862	53.5 (49.6, 57.5)	53.4
Summer	BUI	289	0.957	58.9 (50.0, 67.7)	58.8
All year	DC	861	0.935	222.0 (200.1, 244.0)	221.6
Fall	DC	700	0.466	383.3 (361.6, 405.1)	383.2
Spring	DC	394	0.689	195.9 (185.3, 206.4)	196.2
Summer	DC	853	0.921	234.8 (212.9, 256.7)	234.3
All year	DMC	294	0.978	41.7 (32.9, 50.5)	41.5
Fall	DMC	220	0.773	30.6 (23.0, 38.1)	30.4
Spring	DMC	152	0.815	69.2 (40.8, 74.8)	71.3
Summer	DMC	286	0.980	40.6 (31.8, 49.5)	40.4
All year	FFMC	100	0.997	90.6 (88.2, 93)	90.8
Fall	FFMC	94	0.962	88.4 (86.1, 90.8)	88.3
Spring	FFMC	91	0.936	92.3 (90, 94.6)	92.4
Summer	FFMC	98	0.993	90.4 (88.0, 92.8)	90.7
All year	FWI	81	0.992	22.2 (19.9, 24.5)	22.1
Fall	FWI	69	0.858	16.7 (14.8, 18.6)	16.7
Spring	FWI	63	0.862	24.7 (23.0, 26.4)	24.6
Summer	FWI	79	0.991	21.4 (19.1, 23.8)	21.4
All year	ISI	54	0.969	7.2 (5.4, 9.0)	7.2
Fall	ISI	33	0.909	5.9 (4.8, 7.0)	5.9
Spring	ISI	42	0.720	9.8 (8.7, 11.1)	9.8
Summer	ISI	54	0.976	7.0 (5.2, 8.8)	7.0

in order to avoid overfitting). These models were fitted for the whole study area, as well as for each Ecozone unit for the entire fire season as well as seasonally (i.e., spring, summer and fall). For each model, a ten-fold cross-validation approach (Hastie et al., 2009) was applied to understand the model strength and reliability. Model coefficients as well as both goodness of fit (r-squared value with standard deviations) and root-mean-square deviation (RMSE) are reported. Recommendations for whether a model can produce a reliable reference were determined by visually checking the scatter plot and fitted curve as well as the goodness of fit statistics (e.g., r-squared value and RMSE).

3. Results

3.1. Summary stats

Our comparison of all FWI System indices between spread days and non-spread days by Ecozone show that the majority of indices were significant ($\alpha = 0.05$), and only 16 of 324 were not significant (Table 1). The non-significant cases are almost all by DC, DMC, and BUI primarily in spring and fall for TP, BSE and BC. By FRU, only 60 out of 1200 comparisons were not significant (Table S1). These non-significant pairs are, again, mostly DC, DMC, and BUI (56 out of 60 of them), which are indices that represent deeper fuel layer moisture conditions and available fuel.

For the relationships by FRU between mean FWI System indices for spread days and latitude, elevation, and conifer coverage, we found FFMC, ISI, and FWI show negative correlation with latitude across the country (Table 2). This indicates that as latitude increases, spread days occur under relatively less severe fire weather conditions. The same relationships were found for summer fires in FWI and ISI, and for spring fires in ISI. In addition, we found that elevation has a major positive effect on the FWI System indices, especially for DMC, DC, and BUI both annually and seasonally. That is to say, as elevation increases, spread days tend to occur during days of relatively higher DMC, DC, and BUI, i.e., more severe drought conditions.

Results of the correlation tests performed for the mountain areas show very different patterns (Table S2). We found that the mean fire weather

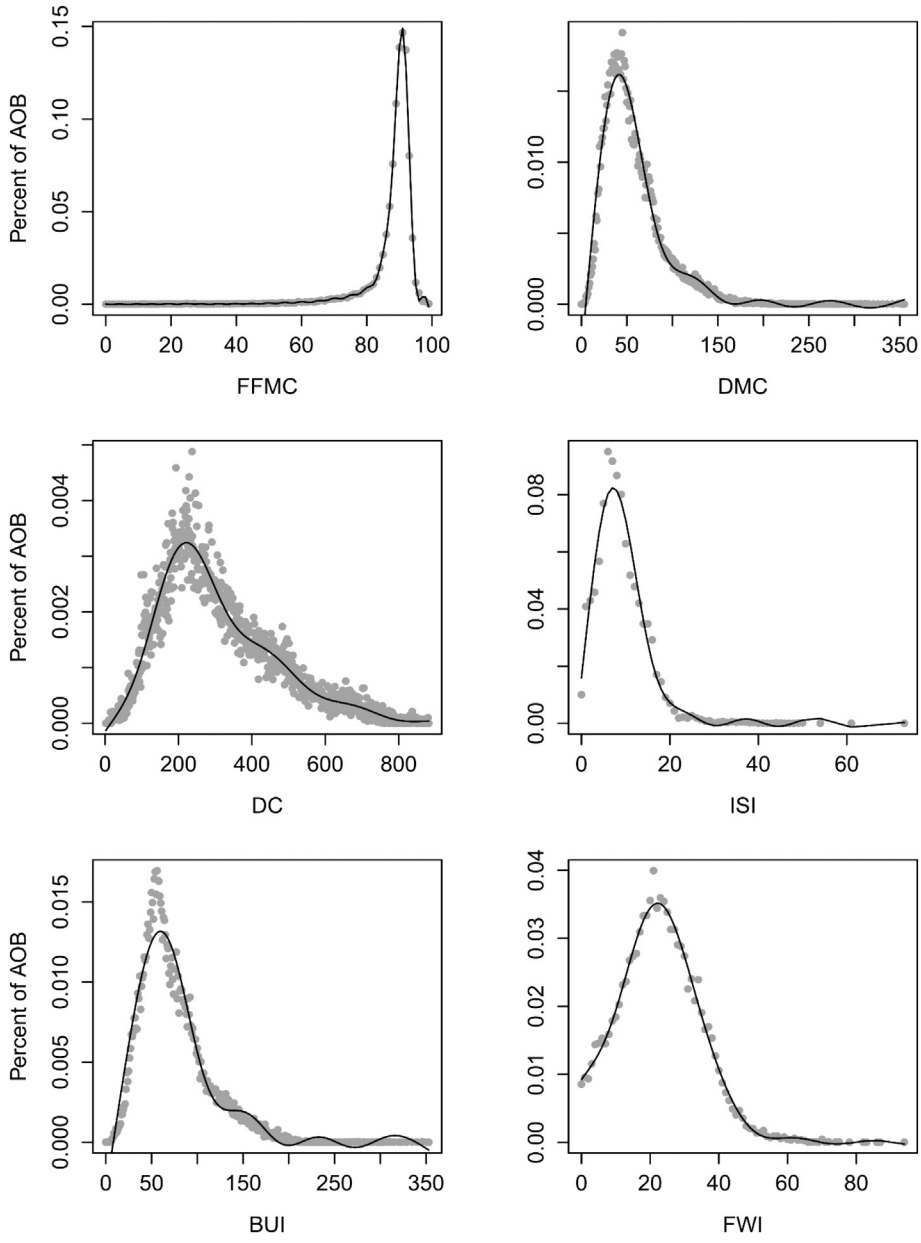

Fig. 2. Proportion of total area burned by each unit FWI System variables summarized over the study area based on fires considered in the study between 2001 and 2019.

conditions (all six FWI System indices, except for ISI) of spread days were positively correlated with conifer coverage but negatively correlated with latitude. This is a surprising result that will be addressed in the Discussion section. Elevation, on the other hand, showed no significant correlations except for ISI over the year and for FWI and ISI in the fall (positively correlated).

For the non-mountainous areas, nine out of the 12 FWI spread day means explored were significantly correlated with conifer coverage (Table S3). These negative correlations indicate that with the increase of conifer coverage, the required fire weather condition (mainly DMC, DC, and BUI, and in one case FWI) for a spread day to occur decreases, opposite to what we found in the mountain area for the same FWI System indices. In addition, DC was found to be significantly and positively correlated with latitude for both the whole fire season and the fall; this indicates that spread days occur under drier conditions in higher latitudes as day-length shortens in the fall. Surprisingly, mean ISI of spread days at various FRUs was found to be positively correlated with elevation but not with conifer coverage. FFMC was found to have no significant correlations with any of the factors considered.

3.2. Fire weather conditions that support the most area burned

FWI System indices showed strong nonlinear relationships with area burned across the study area (Table 3; Fig. 2; Figs. S1, S2, and S3). The annual FWI System index values at which the most area burned were found to be very similar to that of the summer (Table 3). These values tend to be higher in the spring, except for DC and BUI, and lower in the fall, except for DC, relative to the annual values, which corresponds to the general seasonal trend in the DC (McAlpine, 1990). Most noteworthy is that high area burned cases occurred primarily within a smaller range of index values both annually (Table 3; Fig. 2) and seasonally (Figs. S1, S2, and S3). This same pattern was also found by ecozone (Table 4; Table S4).

Within Ecozones (Table 4), we found that FFMC varied the least (coefficient of variation (CV) = 0.015) with maximum values typically between 88 and 92. This was followed by FWI and DMC with CV = 0.25 and 0.30, respectively, with DC varying the most (CV = 0.39). Similarly, strong nonlinear relationships between FWI System indices and the corresponding area burned were also found at the ecozone level (Table 4; Table S4), especially for FFMC (Fig. S4), ISI (Fig. S5), and FWI (Fig. S6). Similar to the full study area analysis, the annual FWI System indices values for which the most area burned were again found to be very similar to those in the summer. Due to limitations of sample size, results for some ecozones at various seasons are either missing or not reliable; this is most notable in the spring and fall seasons (Table S4). However, a few ecozones did show some seasonal variations, especially in ISI and FWI. For example, within the BSW ecozone, ISI was 8.7 for spring, 7.4 for summer, and 6.6 for the fall, while FWI was 26.3, 21.0, and 16.8 for each of the three seasons respectively (Table S4). For the BC ecozone, the pattern is a bit different; we do see a decrease in ISI from spring to the fall (6.5, 6.0, and 5.4), but FWI values increase from 13.9 in the spring, to 15.5 in the summer, and to 17.8 in the fall. Each ecozone can show different changes over seasons (Table S4), which may reflect the impacts of short-term or long-term fire weather influences and each may deserve their own explanations accordingly.

3.3. Modeling the probability of spread day occurrence

Modeling the probability of spread day occurrence based on single daily FWI System indices allows us to identify spread days more accurately. Models developed based on all fires for all seasons collected over the country (Table 5 for model coefficients) show a higher goodness of fit (measured by r-squared values) in FFMC, ISI, and FWI annually (Table 5; Fig. 3). The otherwise strong relationships of DMC, DC, and BUI with spread day occurrence deteriorated at certain points, e.g., around 150 for both DMC and DC, and close to 200 for BUI (Fig. 3), an indication of losing association between the occurrence of spread day and fuel dryness and availability. Similar patterns can also be found when modeling by season (e.g., Figs. S7, S8, and S9).

Table 4
FWI System variable values at which the most area burned (Max) determined based on the GAMs for all season combined by ecozone. We also report mean (min, max) FWI System variable values of the top 5 % (top5pc) most area burned cases. A mean value of the top5pc will be used for Max if the GAM model changes monotonically by visually checking the fitted curves, and were marked * for caution.

Ecozone	Indices	Sample size	r^2_{adj}	top5pc	Max
BC	FFMC	91	0.971	89.7 (87.3, 92.0)	89.8
BP	FFMC	99	0.944	91.7 (89.2, 94.1)	91.9
BSE	FFMC	92	0.967	90.7 (88.4, 93.0)	90.8
BSW	FFMC	99	0.981	91.0 (88.6, 93.4)	91.2
HP	FFMC	85	0.958	90.6 (88.4, 92.8)	90.8
MC	FFMC	92	0.973	91.8 (89.5, 94.1)	92.2
PM	FFMC	81	0.521	90.8 (88.7, 93.0)	90.8*
TC	FFMC	88	0.885	87.8 (85.6, 90.0)	87.9
TP	FFMC	96	0.962	89.8 (87.4, 92.2)	90.0
TSE	FFMC	81	0.959	90.2 (88.0, 92.3)	90.2
TSW	FFMC	92	0.921	90.4 (88.2, 92.8)	90.7
BC	DMC	156	0.91	33.5 (29.4, 37.5)	33.4
BP	DMC	154	0.887	41.0 (37.1, 45.0)	40.9
BSE	DMC	104	0.927	38.8 (36.0, 41.7)	38.8
BSW	DMC	178	0.954	40.1 (35.5, 44.8)	40.1
HP	DMC	109	0.768	41.2 (38.4, 44.1)	41.3
MC	DMC	294	0.892	68.4 (59.6, 77.3)	68.4
PM	DMC	96	0.403	38.0 (35.5, 40.6)	38.1
TC	DMC	137	0.872	26.3 (22.7, 29.9)	26.1
TP	DMC	176	0.94	48.9 (44.5, 53.4)	48.9
TSE	DMC	84	0.855	23.6 (21.4, 25.8)	23.6
TSW	DMC	191	0.964	49.3 (44.2, 54.3)	49.2
BC	DC	622	0.537	281.6 (265.5, 297.6)	281.7
BP	DC	693	0.761	205.8 (186.1, 225.4)	205.2
BSE	DC	326	0.665	182.3 (172.2, 192.4)	182.6
BSW	DC	545	0.901	247.0 (232.9, 261.1)	246.8
HP	DC	463	0.409	226.3 (213.8, 238.8)	226.5
MC	DC	804	0.825	481.2 (459.3, 503.2)	481.3
PM	DC	320	0.026	231.0 (217.2, 244.8)	230.9
TC	DC	502	0.649	302.8 (290.1, 315.4)	302.8
TP	DC	841	0.602	423.1 (401.3, 445.0)	423.8
TSE	DC	256	0.574	106.4 (99.4, 113.5)	106.4
TSW	DC	720	0.708	274.2 (255.6, 292.8)	274.1
BC	ISI	26	0.956	6.0 (5.3, 6.6)	6.0
BP	ISI	37	0.819	8.3 (7.1, 9.5)	8.2
BSE	ISI	42	0.905	9.9 (8.7, 11.1)	9.9
BSW	ISI	41	0.943	7.4 (6.3, 8.5)	7.4
HP	ISI	41	0.882	10.0 (8.7, 11.3)	10.0
MC	ISI	33	0.941	7.6 (6.8, 8.4)	7.6
PM	ISI	11	0.435	5.3 (5.1, 5.6)	5.3
TC	ISI	17	0.987	3.3 (2.9, 3.6)	3.2
TP	ISI	28	0.984	6.5 (5.8, 7.2)	6.6
TSE	ISI	47	0.907	11.3 (9.5, 13.1)	11.3
TSW	ISI	43	0.973	7.0 (5.8, 8.2)	7.0
BC	BUI	176	0.895	45.2 (40.6, 49.9)	45.0
BP	BUI	159	0.893	57.0 (53.1, 61.0)	56.8
BSE	BUI	108	0.907	49.6 (46.7, 52.5)	49.6
BSW	BUI	175	0.971	56.9 (52.3, 61.5)	56.9
HP	BUI	118	0.878	57.0 (54.0, 60.1)	57.1
MC	BUI	299	0.878	103.1 (94.3, 111.9)	103.0
PM	BUI	116	0.332	54.8 (51.6, 58.0)	54.9
TC	BUI	141	0.801	50.0 (46.4, 53.5)	49.8
TP	BUI	204	0.879	70.7 (65.4, 76)	70.5
TSE	BUI	91	0.894	30.5 (28.1, 32.9)	30.5
TSW	BUI	205	0.944	71.4 (66.2, 76.7)	71.5
BC	FWI	46	0.868	15.7 (14.4, 16.9)	15.7
BP	FWI	63	0.904	23.4 (21.6, 25.1)	23.3
BSE	FWI	62	0.88	22.9 (21.1, 24.8)	23.0
BSW	FWI	66	0.972	22.0 (20.1, 24.0)	22.0
HP	FWI	70	0.722	23.0 (20.9, 25.2)	23.0
MC	FWI	73	0.925	28.3 (26.5, 30.0)	28.3
PM	FWI	32	0.656	14.8 (13.9, 15.6)	14.8
TC	FWI	38	0.874	9.7 (8.8, 10.6)	9.7
TP	FWI	57	0.955	21.1 (19.6, 22.5)	21.0
TSE	FWI	64	0.937	19.8 (17.5, 22.1)	19.8
TSW	FWI	73	0.964	24.0 (22.1, 25.9)	24.0

* Mean value of the top5pc 90.8 was used here due to the monotonic change (see Fig. S4).

Table 5
Thresholds of FWI System variables for the occurrence of spread days at a probability of 50 % (p50), for the whole study area. A semi-binomial regression model was used, and adjusted r-square and sample size for each model were also reported in the table. NA indicates the curve never reached the probability thresholds used in the table. By visually comparing with fitted curves, we also identified models that should not be used (marked * in the column "p50").

Season	Indices	Intercept	x	x^2	r^2(±sd)	RMSE	Sample size	p50
All year	BUI	−1.64201	0.020627	−4.80E-05	0.29 (0.17)	0.23	299	105.5
Fall	BUI	−2.53066	0.017155	−3.01E-05	0.23 (0.12)	0.24	249	NA*
Spring	BUI	−1.57074	0.04877	−0.00017	0.79 (0.17)	0.11	154	36.8
Summer	BUI	−1.75973	0.022903	−5.30E-05	0.35 (0.17)	0.22	289	100.0
All year	DC	−0.39641	−0.00198	3.03E-06	0.14 (0.14)	0.15	861	813.3*
Fall	DC	−0.64521	−0.00311	2.16E-06	0.05 (0.05)	0.19	700	NA*
Spring	DC	−0.94639	0.01075	−1.10E-05	0.54 (0.54)	0.15	394	97.8
Summer	DC	−0.53102	−0.00164	3.41E-06	0.27 (0.27)	0.15	853	702.6*
All year	DMC	−1.23338	0.019859	−4.92E-05	0.21 (0.13)	0.25	294	76.7
Fall	DMC	−2.23392	0.020206	−4.77E-05	0.18 (0.14)	0.26	220	NA*
Spring	DMC	−1.40665	0.04908	−0.00017	0.77 (0.15)	0.11	152	32.2
Summer	DMC	−1.34145	0.022379	−5.58E-05	0.29 (0.21)	0.25	286	73.4
All year	FFMC	−2.16869	−0.08044	0.001197	0.93 (0.07)	0.05	100	87.8
Fall	FFMC	−3.85961	−0.09843	0.001492	0.77 (0.36)	0.04	94	93.6
Spring	FFMC	−0.79398	−0.08845	0.001189	0.8 (0.23)	0.12	91	82.5
Summer	FFMC	−2.14468	−0.07103	0.001063	0.89 (0.17)	0.06	98	89.4
All year	FWI	−1.49281	0.077487	−0.00019	0.94 (0.05)	0.07	81	20.3
Fall	FWI	−2.17822	0.033473	0.000817	0.89 (0.1)	0.12	69	35.1
Spring	FWI	−1.57986	0.147955	−0.00078	0.97 (0.05)	0.04	63	11.4
Summer	FWI	−1.45708	0.076685	−0.00022	0.93 (0.05)	0.07	79	20.2
All year	ISI	−1.03833	0.136841	−0.00082	0.85 (0.3)	0.09	54	8.0
Fall	ISI	−2.28863	0.134799	0.002955	0.95 (0.09)	0.10	33	13.2
Spring	ISI	−1.06914	0.243153	−0.00341	0.81 (0.3)	0.09	42	4.7
Summer	ISI	−0.87771	0.117325	−0.00075	0.8 (0.33)	0.12	54	7.9

Models developed by ecozone (Table S5 for model coefficients) corroborated that FFMC, ISI, and FWI are the stronger predictors of probability of spread day occurrence (Table 6; Figs. S10, S11, and S12), while DC is usually the weakest. These findings were consistent when modeling within seasons as well, where sample sizes permitted us to do so (Table S5). Similarly, each ecozone may show different seasonal fire weather thresholds where there is a 50 % chance that a spread day occurs; however, these values may not necessarily coincide with the most area burned fire weather values shown in the previous analysis.

Overall, FFMC, ISI, and FWI are shown to be the stronger predictors for the occurrence of spread days regardless of the spatial partitions of the study area. In comparison, the other FWI System variables, especially DC showed very poor predictive power (Tables 5 & 6; Table S4).

In comparison, FWI System variable values corresponding to the maximum area burned at both national and ecozone levels are higher than those obtained through the semi-binomial regression models (Fig. 4). Their spatial variations also differ although both approaches resulted in quite homogenous FFMC values across ecozones, with the only difference being that those values corresponding to the maximum area burned (Fig. 4A) are generally higher. In comparison of the spatial variations of ISI, the spatial changes are quite similar in the west but opposite in the east, particularly for TSE and BSE (Fig. 4B and E). FWI showed similar patterns to what we found in ISI, particularly for TSE and BSE (Fig. 4C and F).

4. Discussion

The spread day is an important concept for understanding the relationship between fire weather conditions and some of the major fire regime characteristics, including fire sizes (e.g., Parisien et al., 2013; Wang et al., 2020), annual area burned, and fire frequency (Wang et al., 2021, 2022). For example, the power relationship between area burned and duration of burning (McArthur, 1968; Van Wagner, 1969; Rothermel et al., 1994) can only be achieved when the duration is measured by the number of spread days (e.g., Wang et al., 2020). It is also critical for fire management to identify thresholds that may indicate the potential for dangerous fire spreading events (e.g., Podur and Wotton, 2011; Hanes et al., 2022).

In this study, we explored relationships between changes in the mean spread day fire weather condition when considering spatial location, conifer coverage, and elevation. We then used two different approaches to characterize and model the occurrence of spread days based on fire weather conditions. We found that spread day fire weather conditions decrease with the increase of latitude across the country. We suspect that the increased day-length in summer and spring may increase the burning period, which may in turn lower the thresholds for a spread day (see also Clarke et al., 2022). Additionally, within the non-mountainous areas of Canada, we found that conifer coverage has a major influence, as when conifer coverage increases, the severity of fire weather conditions associated with a spread day decrease (i.e., fires spread easier at lower indices with greater conifer coverage). We also found a strong non-linear relationship between the FWI System index values and area burned. These relationships are especially strong for FFMC, ISI, and FWI over the whole range of observations. These relationships were also strong for DMC, DC, and BUI below certain thresholds, but became unpredictable beyond. This might be an indication that spread days are not limited by these factors. Similarly, the prediction models of spread day occurrence show strong predictive power by FFMC, ISI, and FWI, but are weaker for DMC, DC, and BUI (see also McAlpine, 1995). These findings are logical, as FFMC, ISI, and FWI are often associated with fire spread and intensity, whereas DMC, DC, and BUI are often associated with fuel availability and consumption (Van Wagner, 1987).

We used GAMs to model the relationship between FWI System indices and associated area burned. By identifying the FWI System index values that support the most burned area, we could potentially identify FWI System index spread day thresholds without having to rigidly define spread days a priori. The thresholds found in this analysis may therefore be considered more objective in comparison. The FWI System indices ranging for the top 5 % most area burned cases may add some flexibility when used as indicators of spread days. The semi-binomial regression models built to predict the probability of a spread day occurrence could also be used to make inferences of the critical FWI System indices thresholds for a spread day (e.g., FWI System indices values at $p = 50$ %). However, because a spread day must be quantified/defined (e.g., at least 1 m min^{-1} with a spread distance exceeding 240 m a day in this study) prior to the establishment of the models, these spread day thresholds may need to vary with the criteria used to define a spread day, a clear limitation from this perspective. Such models would be better used to model the probabilistic distribution of

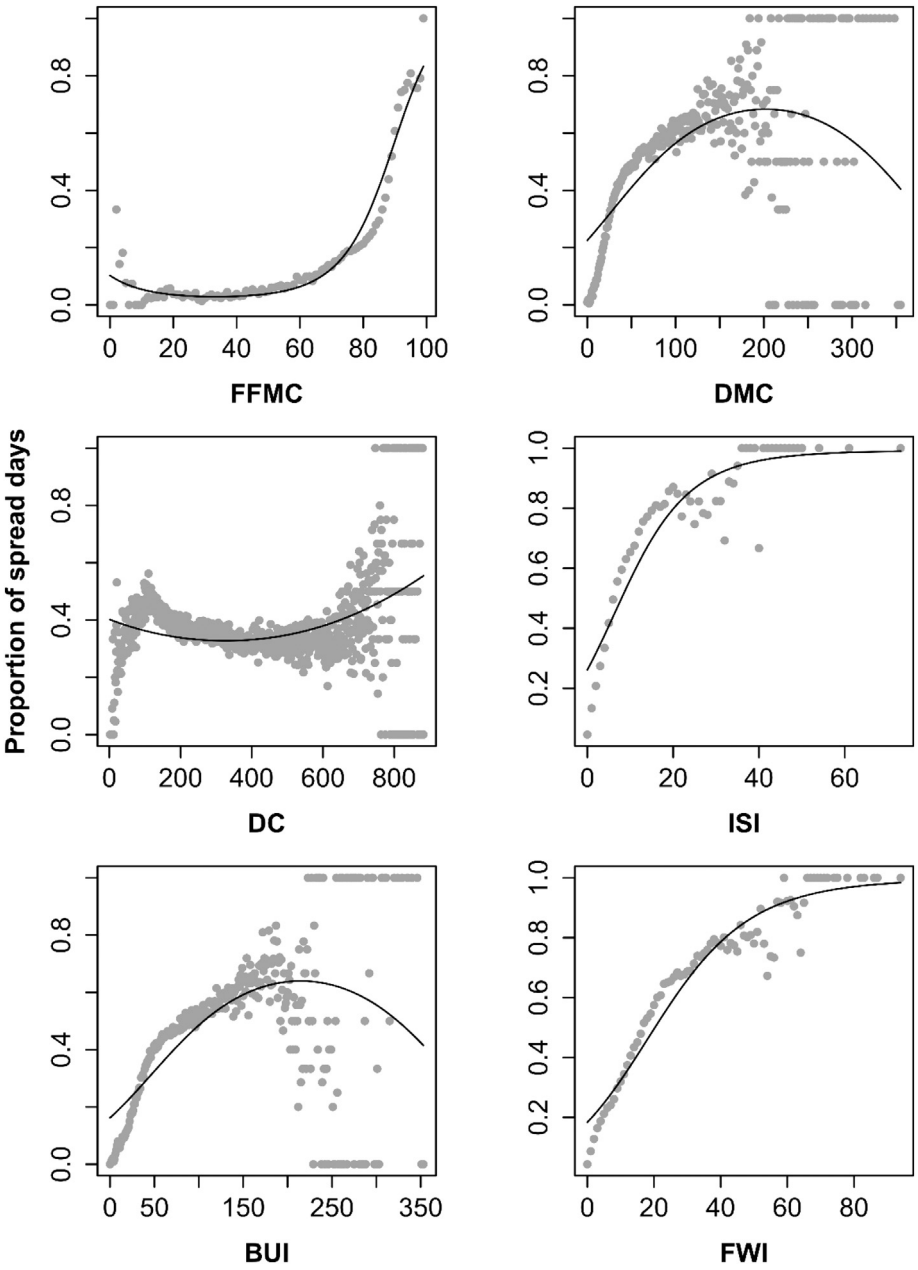

Fig. 3. Probability of spread days occurrence modeled by FWI System variable for the whole study area. The deterioration of BUI, DMC and DC at certain thresholds is an indication of the losing association between fuel availability and the occurrence of spread day.

a spread day over a specific FWI System index for a specific area, which may improve our understanding of how fire-conducive weather conditions change over time or space (see also Podur and Wotton, 2011). For these reasons, we recommend the first approach (i.e., GAMs) for the identification of spread day thresholds.

Comparing our results with those of other recently proposed extreme fire weather conditions, we found some discrepancies. For example, in Hanes et al. (2022), they found the extreme fire weather condition measured by FFMC also had the highest proportion of area burned for FFMC >90 for Ontario, similar to what we found in this study. Although they were relating FFMC to the probability of sustainable flaming ignition, not spread rate directly, fire managers often use it as an indicator of surface fire rate of spread (Hanes et al., 2022). The ISI thresholds in that paper, which were associated with rate of spread, were not denoted as extreme until ISI > 10, whereas the ISI values indicative of a spread day in our study were typically lower. Overall, FFMC values were the most consistent spatially in comparison to the other FWI System indices, which leads us to recommend FFMC as the indicator of choice for spread days if only one FWI System index is used. FWI was found to be less variable than the remaining indices; however, because of the power relationship between FWI and fire energy release (Van Wagner, 1987), it might not be the best candidate to choose for the whole study area as a small variation in the index may indicate a more important difference. This leads us to recommend ISI as the second choice; however, using a single value of this index for a large area would still be quite biased to specific regions (e.g., northern Canada). Although the calculation of FFMC involves wind speed, it is a measurement of fine fuel moisture condition, which won't immediately respond to wind speed changes due to the drying time-lag (Van Wagner, 1987); ISI, on the other hand, is the combination of FFMC and wind, and will respond to the change of wind speed directly in its calculation. FFMC being more consistent than ISI may suggest that fuel moisture is the critical element, as fuel moisture determines if the fire will ignite and spread, also

Table 6
Thresholds of FWI System variables for the occurrence of spread days at a probability of 50 % (p50) with all season combined by Ecozone. A semi-binomial regression model was used, and adjusted r-square and sample size for each model were also reported in the table. NA indicates the curve never reached the probability thresholds used in the table. By visually comparing with the fitted curves, we also identified models that should not be used (marked * in the column "p50").

Ecozone	Indices	Intercept	x	x^2	r^2(± sd)	RMSE	Sample size	p50
BC	FFMC	−3.45713	−0.04815	0.000992	0.94 (0.06)	0.07	91	88.1
BP	FFMC	−3.04774	−0.07538	0.001239	0.88 (0.11)	0.08	99	88.6
BSE	FFMC	−3.13298	−0.02275	0.000711	0.90 (0.09)	0.07	92	84.3
BSW	FFMC	−0.63622	−0.13585	0.001685	0.78 (0.28)	0.11	99	85.1
HP	FFMC	−1.07864	−0.10226	0.001311	0.75 (0.28)	0.09	85	87.4
MC	FFMC	−4.4371	0.000533	0.000498	0.94 (0.04)	0.05	92	93.8
PM	FFMC	−3.97421	−0.05615	0.001099	0.79 (0.22)	0.07	81	90.9
TC	FFMC	−4.07093	0.008174	0.000463	0.94 (0.04)	0.05	88	85.4
TP	FFMC	−2.7287	−0.0853	0.00134	0.94 (0.06)	0.06	96	87.1
TSE	FFMC	0.283215	−0.09993	0.001153	0.53 (0.24)	0.16	81	83.7
TSW	FFMC	−4.64324	−0.03329	0.000992	0.97 (0.03)	0.05	92	87.2
BC	DMC	−2.98677	0.081107	−0.00045	0.56 (0.19)	0.18	156	51.7
BP	DMC	−2.54764	0.046019	−0.00012	0.73 (0.16)	0.16	154	67.2
BSE	DMC	−2.45476	0.097562	−0.00062	0.49 (0.26)	0.24	104	31.5
BSW	DMC	−2.43156	0.066599	−0.00028	0.66 (0.15)	0.16	178	45.1
HP	DMC	−2.04249	0.054117	−0.00021	0.59 (0.28)	0.19	109	45.9
MC	DMC	−1.57897	0.018664	−4.04E-05	0.24 (0.12)	0.25	294	111.5
PM	DMC	−2.10253	0.059909	−0.00046	0.18 (0.17)	0.26	96	NA
TC	DMC	−1.9703	0.05538	−0.0003	0.46 (0.26)	0.18	137	48.1
TP	DMC	−2.55436	0.054131	−0.00021	0.79 (0.19)	0.11	176	61.9
TSE	DMC	−1.86943	0.085629	−0.0005	0.71 (0.26)	0.15	84	25.7
TSW	DMC	−1.94765	0.033263	−5.98E-05	0.82 (0.13)	0.12	191	66.5
BC	DC	−0.81427	−0.00026	−3.87E-07	0.03 (0.03)	0.14	622	NA*
BP	DC	−0.84051	0.003396	−1.01E-05	0.55 (0.17)	0.11	693	NA*
BSE	DC	−1.36635	0.009069	−8.35E-06	0.32 (0.18)	0.24	326	180.8*
BSW	DC	−1.29255	0.006402	−1.05E-05	0.11 (0.06)	0.15	545	NA*
HP	DC	0.683086	−0.00739	9.85E-06	0.17 (0.14)	0.21	463	108.1*
MC	DC	−2.07663	0.007604	−8.52E-06	0.28 (0.17)	0.16	804	NA*
PM	DC	0.715983	−0.01269	2.36E-05	0.08 (0.07)	0.35	320	64.1*
TC	DC	−0.57789	0.006363	−1.81E-05	0.29 (0.10)	0.18	502	NA*
TP	DC	−0.10053	−0.00444	6.66E-06	0.30 (0.17)	0.18	841	689.1*
TSE	DC	2.191238	−0.02656	6.71E-05	0.35 (0.18)	0.2	256	117.2*
TSW	DC	0.251411	−0.00306	2.24E-06	0.18 (0.09)	0.15	720	87.9
BC	ISI	−1.67671	0.265646	−0.00314	0.77 (0.37)	0.15	26	6.9
BP	ISI	−1.82225	0.231462	−0.00319	0.75 (0.31)	0.15	37	9.0
BSE	ISI	−1.30676	0.219074	−0.0017	0.88 (0.28)	0.05	42	6.3
BSW	ISI	−1.52552	0.210231	0.000509	0.99 (0.01)	0.04	41	7.1
HP	ISI	−0.88748	0.084117	−9.05E-05	0.69 (0.32)	0.16	41	10.7
MC	ISI	−1.28423	0.128926	−0.00085	0.83 (0.23)	0.14	33	10.7
PM	ISI	−2.6282	0.596589	−0.0193	0.99 (0.02)	0.2	11	5.3
TC	ISI	−1.5372	0.383699	−0.01281	0.74 (0.40)	0.11	17	4.8
TP	ISI	−1.82706	0.26278	−0.00104	0.98 (0.02)	0.06	28	7.2
TSE	ISI	−0.40351	0.107233	−0.00076	0.65 (0.37)	0.17	47	3.9
TSW	ISI	−1.13026	0.1553	−0.00202	0.64 (0.39)	0.17	43	8.1
BC	BUI	−2.67493	0.045747	−0.00017	0.48 (0.16)	0.18	176	86.7
BP	BUI	−3.12759	0.046889	−0.00013	0.82 (0.13)	0.11	159	88.7
BSE	BUI	−3.10246	0.102996	−0.00061	0.65 (0.21)	0.19	108	39.1
BSW	BUI	−3.16166	0.069457	−0.00028	0.68 (0.12)	0.16	175	59.6
HP	BUI	−3.48929	0.103327	−0.0007	0.53 (0.26)	0.17	118	51.9
MC	BUI	−1.87731	0.018355	−3.70E-05	0.29 (0.18)	0.23	299	144.1
PM	BUI	−2.94834	0.074146	−0.00048	0.26 (0.13)	0.23	116	NA*
TC	BUI	−2.21799	0.049434	−0.00024	0.39 (0.21)	0.2	141	65
TP	BUI	−2.85296	0.043527	−0.00012	0.75 (0.18)	0.13	204	87.5
TSE	BUI	−1.82774	0.064143	−0.00033	0.59 (0.33)	0.19	91	34.6
TSW	BUI	−2.43702	0.036565	−9.07E-05	0.77 (0.14)	0.13	205	84.2
BC	FWI	−2.02636	0.128508	−0.00042	0.98 (0.03)	0.05	46	16.7
BP	FWI	−2.74621	0.160706	−0.00139	0.84 (0.27)	0.11	63	20.8
BSE	FWI	−1.47454	0.132429	−0.0008	0.91 (0.10)	0.07	62	12
BSW	FWI	−1.7786	0.121968	−0.00061	0.97 (0.05)	0.05	66	15.8
HP	FWI	−1.19252	0.046851	0.000194	0.75 (0.25)	0.15	70	23.2
MC	FWI	−1.41388	0.035923	0.000373	0.86 (0.12)	0.1	73	30
PM	FWI	−3.31716	0.423617	−0.01176	0.87 (0.16)	0.13	32	11.5
TC	FWI	−1.67465	0.204819	−0.00436	0.64 (0.35)	0.08	38	10.5
TP	FWI	−2.38152	0.163753	−0.00164	0.86 (0.30)	0.09	57	17.7
TSE	FWI	−0.79184	0.089968	−0.00067	0.51 (0.36)	0.17	64	9.5
TSW	FWI	−1.99022	0.11642	−0.00076	0.94 (0.07)	0.06	73	19.6

influencing spot fire ignition potential (e.g., Flannigan et al., 2016; Nolan et al., 2016; Ellis et al., 2022). The GAMs and semi-binomial regression models were not presented at the FRU level because most of the units did not have sufficient samples to build these models.

In this study, we found that the mean spread day fire weather conditions showed a positive correlation with conifer coverage in the mountain areas (Table S2), which indicates that more severe fire weather conditions are required for a spread day to occur in denser conifer areas. This is contrary

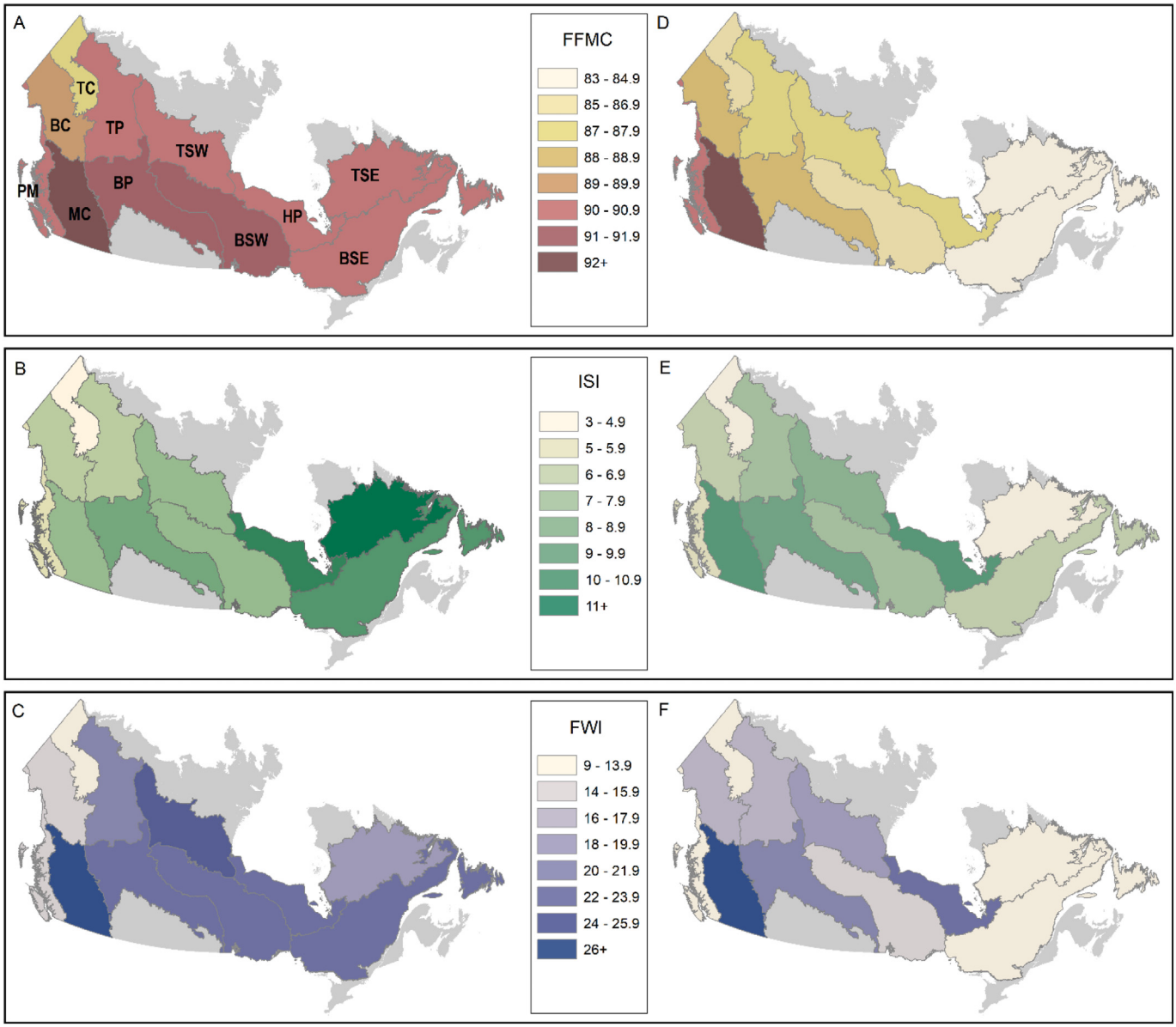

Fig. 4. FWI System variable thresholds corresponding the most area burned (A, B, and C) and FWI System variable thresholds corresponding to 50 % probability for a spread day to occur (D, E, and F).

to the non-mountainous areas, where it was found that as conifer coverage increases, less severe fire weather conditions are needed for a spread day to occur. A further examination showed that conifer coverage is also positively correlated with fire weather conditions for non-spread days. This may indicate that, overall, more severe fire weather conditions are required to sustain fires in the mountain areas, where conifer forests are more prevalent at higher elevation. In addition, snow melt in higher elevation is also later than that in lower elevation, and it takes more time to dry out. Secondly, we suspect that fire growth in the mountain areas was underestimated as the fire growth delineation (and therefore the identification of spread days) does not account for the added distance that a slope creates (i.e., a bigger run on a slope is required to equal the same distance on a flat surface) (Parks, 2014). Future fire growth delineation models should take slope/elevation into account and a more detailed or finer scale approach to determining FWI thresholds is required in mountain areas because of the varying elevation and the subsequent fuels and fire weather conditions that result from it.

The reliability of our results from this study depends heavily on the quality of both fire growth delineation (e.g., Parks, 2014; Hall et al., 2020) and the fire weather data (i.e., gridded fire weather database (McElhinny et al., 2020)). Although both the fire growth modeling technique and fire weather database were well validated and tested, there is still room for improvement. Limitations exist in both, and these limitations are certainly reflected in our results. For example, besides the potential impacts of smaller sample size, the lower FWI thresholds for a spread day to occur in the western mountainous ecozones (i.e., TC, PM, and BC) might in part be caused by the relatively coarse resolution (~30 km) ERA5 dataset. This may be improved with better data in the future. In addition, the threshold of defining a spread day adopted in this study does affect the inference of the fire weather condition for spread days in the probability models. Therefore, future research should focus on how to properly quantify and identify a spread day for in situ fire events. Future research should also investigate thresholds of spread days by both hot-dry-windy index (Srock et al., 2018; McDonald et al., 2018) and vapor pressure deficit (Sedano and Randerson, 2014; Clarke et al., 2022) in the forested area of Canada. In addition, research aiming at better understanding of the relationship between fire weather condition and fire spread, e.g., the relationship between atmospheric instability and fire growth or identifying

top-down and bottom-up factors affecting spread days, should also be promoted.

5. Conclusion

Making the link between fire weather potential and fire spread events on the ground is crucial for both our understanding of fire regime changes and for fire management (e.g., fire preparedness). By examining the paired fire weather condition and daily fire growth, we found that the fire weather conditions for a spread day to occur change over seasons and regions. Spread day fire weather conditions correlated negatively with latitude and conifer coverage in the study area and the non-mountainous areas of Canada, respectively; but correlated positively with conifer coverage in the Rocky Mountain area. Using generalized additive models (GAMs) and semi-binomial regression models, this paper explored the fire weather indicators for a spread day, a day when fires grow a significant amount of area. We found that among the six FWI System indices, FFMC, ISI, and FWI show stronger predictive power in both modeling approaches in terms of identifying a spread day and predicting the occurrence of spread days. FFMC was the most consistent across all spatial and temporal scales.

CRediT authorship contribution statement

XW, SE, and MF conceived the research idea, JO and TS compiled the data, XW and TS performed the analysis, and XW, TS, CH, and MF wrote the paper.

Data availability

Data will be made available on request.

Declaration of competing interest

The authors declare no conflicts of interest and no competing interests.

Acknowledgement

We thank Dr. Piyush Jain from Canadian Forest Service for providing the additional ERA5 outputs. This research was partially funded by two Canadian Safety and Security Program grants to X.W. (CSSP-2016-CP-2286 and CSSP-2018-TI-2406).

Appendix A. Supplementary data

Supplementary data to this article can be found online at https://doi.org/10.1016/j.scitotenv.2023.161831.

References

Abatzoglou, J.T., Battisti, D.S., Williams, A.P., Hansen, W.D., Harvey, B.J., Kolden, C.A., 2021. Projected increases in western US forest fire despite growing fuel constraints. Commun. Earth Environ. 2 (1), 1–8.

Barber, Q.E., Parisien, M.-A., Whitman, E., Stralberg, D., Johnson, C.J., St-Laurent, M.-H., DeLancey, E.R., Price, D.T., Arseneault, D., Wang, X., Flannigan, M.D., 2018. Potential impacts of climate change on the habitat of boreal woodland caribou. Ecosphere 9 (10), e02472. https://doi.org/10.1002/ecs2.2472.

Cai, X., Wang, X., Jain, P., Flannigan, M.D., 2019. Evaluation of gridded precipitation data and interpolation methods for forest fire danger rating in Alberta, Canada. J. Geophys. Res. Atmos. 124, 3–17. https://doi.org/10.1029/2018JD028754.

Clarke, H., Nolan, R.H., De Dios, V.R., Bradstock, R., Griebel, A., Khanal, S., 2022. Boer MM 2022 Forest fire threatens global carbon sinks and population centres under rising atmospheric water demand. Nat. Commun. 13, 7161. https://doi.org/10.1038/s41467-022-34966-3.

Coop, J.D., Parks, S.A., Stevens-Rumann, C.S., Ritter, S.M., Hoffman, C.M., 2022. Extreme fire spread events and area burned under recent and future climate in the western USA. Glob. Ecol. Biogeogr. 00, 1–11.

Copernicus Climate Change Service (C3S), 2017. ERA5: Fifth generation of ECMWF atmospheric reanalyses of the global climate, Copernicus Climate Change Service Climate Data Store (CDS). available at: https://cds.climate.copernicus.eu/cdsapp#!/home (last access: 17 May 2019).

Ecological Stratification Working Group (ESWG), 1996. A National Ecological Framework for Canada. Agriculture and Agri-Food Canada and Environment Canada, Ottawa.

Ellis, T.M., Bowman, D.M.J.S., Jain, P., Flannigan, M.D., Williamson, G.J., 2022. Global increase in wildfire risk due to climate-driven declines in fuel moisture. Glob. Chang. Biol. 28, 1544–1559. https://doi.org/10.1111/gcb.16006.

Erni, S., Wang, X., Taylor, S.W., Boulanger, Y., Swystun, T., Flannigan, M.D., Parisien, M.-A., 2020. Developing a two-level fire regime zonation system for Canada. Can. J. For. Res. 50 (3), 259–273.

Flannigan, M.D., Wotton, B.M., Marshall, G.A., de Groot, W.J., Johnston, J., Jurko, N., Cantin, A.S., 2016. Fuel moisture sensitivity to temperature and precipitation: climate change implications. Clim. Chang. 134, 59–71. https://doi.org/10.1007/s10584-015-1521-0.

Forestry Canada Fire Danger Group, 1992. Development and Structure of the Canadian Forest Fire Behavior Prediction System. Forestry Canada, Ottawa, Ontario Information Report ST-X-3 63 p.

Hall, R.J., Skakun, R.S., Metsaranta, J.M., Landry, R., Fraser, R.H., Raymond, D., Gartrell, M., 2020. Decker V and little J 2020 generating annual estimates of forest fire disturbance in Canada: the national burned area composite. Int. J. Wildland Fire 29, 878–891. https://doi.org/10.1071/WF19201.

Hanes, C.C., Jain, P., Flannigan, M.D., Fortin, V., Roy, G., 2017. Evaluation of the Canadian precipitation analysis (CaPA) to improve forest fire danger rating. Int. J. Wildland Fire 26 (6), 509–522. https://doi.org/10.1071/WF16170.

Hanes, C., Wang, X., Jain, P., Parisien, M.-A., Little, J., Flannigan, M.D., 2019. Fire regime changes in Canada over the last half century. Can. J. For. Res. 49 (3), 256–259.

Hanes, C.C., Wotton, B.M., Jurko, N., McFayden, C., 2022. An approach for defining pyhsicically based fire weather index system classes for Ontario. Information Report GLC-0X-19.

Hastie, T.J., Tibshirani, R.J., 1990. Generalized Additive Models. Chapman and Hall, London.

Hastie, T.J., Tibshirani, R.J., Friedman, J.H., 2009. The Elements of Statistical Learning: Data Mining, Inference, and Prediction. 2nd ed. Springer, New York.

Hirsch, K.G., 1996. Canadian Forest Fire Behavior Prediction (FBP) System: User's Guide. Natural Resources Canada, Canadian Forest Service, Northern Forestry Centre, Edmonton, Alberta Special Report 7.

Latham, D.J., Rothermel, R.C., 1993. Probability of Fire-Stopping Precipitation Events. Research note INT 410. USDA Forest Service, Intermountain Research Station, Ogden, UT, USA.

McAlpine, R.S., 1990. Seasonal Trends in the Drought Code Component of the Canadian Forest Fire Weather Index System. Petawawa National Forestry Institute No. Information Report PI-X-97E/F, Petawawa, ON.

McAlpine, R.S., 1995. Testing the effect of fuel consumption on fire spread rate. Int. J. Wildland Fire 5 (3), 143–152.

McArthur, A.G., 1968. The effect of time on fire behaviour and fire suppression problems. 3-6. E.F.S. Manual, S.A. Emergency Fire Services, Keswick, South Australia, pp. 10–13 8.

McDonald, J.M., Srock, A.F., Charney, J.J., 2018. Development and application of a hot-dry-windy index (HDW) climatology. Atmosphere 9, 285. https://doi.org/10.3390/atmos9070285.

McElhinny, M., Beckers, J.F., Hanes, C., Flannigan, M., Jain, P., 2020. A high-resolution reanalysis of global fire weather from 1979 to 2018 – overwintering the drought code. Earth Syst. Sci. Data 12, 1823–1833.

Nolan, R.H., Boer, M.M., Resco de Dios, V., Caccamo, G., Bradstock, R.A., 2016. Large-scale, dynamic transformations in fuel moisture drive wildfire activity across southeastern Australia. Geophys. Res. Lett. 43, 4229–4238. https://doi.org/10.1002/2016GL068614.

Oliver, J.A., Pivot, F.C., Tan, Q., Cantin, A.S., Wooster, M.J., Johnston, J.M., 2022. A machine learning approach to waterbody segmentation in thermal infrared imagery in support of tactical wildfire mapping. Remote Sens. 14 (9), 2262. https://doi.org/10.3390/rs14092262.

Parisien, M.-A., Walker, G.R., Little, J.M., Simpson, B.N., Wang, X., Perrakis, D.D.B., 2013. Considerations for modeling burn probability across landscapes with steep environmental gradients: an example from the Columbia Mountains, Canada. Nat.Hazards 66, 439–462.

Parks, S.A., 2014. Mapping day-of-burning with coarse-resolution satellite fire-detection data. Int. J. Wildland Fire 23, 215–223.

Podur, J.J., Wotton, B.M., 2011. Defining fire spread event days for fire-growth modeling. Int. J. Wildland Fire 20, 497–507.

Richardson, D., Black, A.S., Monselesan, D.P., Risbey, J.S., Squire, D.T., Tozer, C.R., Canadell, J.G., 2021. Increased extreme fire weather occurrence in Southeast Australia and related atmospheric drivers. Weather Clim. Extremes 34, 100397.

Rothermel, R.C., Hartford, R.A., Chase, C.H., 1994. Fire Growth Maps for the 1988 Greater Yellowstone Area fires. Gen. Tech. Report INT-304. USDA, Forest Service, Intermountain Research Station.

Sedano, F., Randerson, J.T., 2014. Vapor pressure deficit controls on fire ignition and fire spread in boreal forest ecosystems. Biogeosciences 11, 1309–1353.

Srock, A.F., Charney, J.J., Potter, B.E., Goodrick, S.L., 2018. The hot-dry-windy index: a new fire weather index. Atmosphere 9, 279. https://doi.org/10.3390/atmos9070279.

Stocks, B.J., Mason, J.A., Todd, J.B., Bosch, E.M., Wotton, B.M., Amiro, B.D., Flannigan, M.D., Hirsch, K.G., Logan, K.A., Martell, D.L., Skinner, W.R., 2002. Large forest fires in Canada, 1959–1997. J. Geophys. Res. Atmos. 107 (D1) FFR-5.

Stralberg, D., Wang, X., Parisien, M.-A., Robinne, F.N., Sólymos, P., Mahon, C.L., Nielsen, S.E., Bayne, E.M., 2018. Wildfire-mediated vegetation change in boreal forests of Alberta, Canada. Ecosphere 9 (3), e02156.

Valero, M.M., Verstockt, S., Rios, O., Pastor, E., Vandecasteele, F., Planas, E., 2017. Flame filtering and perimeter localization of wildfires using aerial thermal imagery. Proceedings of the Thermosense: Thermal Infrared Applications XXXIX, Anaheim, CA, USA. 10214, p. 1021404.

Valero, M.M., Rios, O., Pastor, E., Planas, E., 2018. Automated location of active fire perimeters in aerial infrared imaging using unsupervised edge detectors. Int. J. Wildland Fire 27, 241–256.

Van Wagner, C.E., 1969. A simple fire-growth model. Forestry Chronicle, pp. 103–104.

Van Wagner, C.E., 1977. Conditions for the start and spread of crown fire. Can. J. For. Res. 7, 23–34.
Van Wagner, C.E., 1987. Development and structure of the Canadian forest fire weather index system. Forestry Technical Report 35. Canadian Forest Service, Ottawa.
Wang, X., Parisien, M.-A., Flannigan, M.D., Parks, S.A., Anderson, K.R., Little, J.M., Taylor, S.W., 2014. The potential and realized spread of wildfires across Canada. Glob. Chang. Biol. 20, 2518–2530.
Wang, X., Thompson, D., Marshall, G.A., Tymstra, C., Carr, R., Flannigan, M.D., 2015. Increasing frequency of extreme fire weather in Canada with climate change. Clim. Chang. 130, 573–586.
Wang, X., Parisien, M.-A., Taylor, S.W., Perakis, D.D., Little, J.M., Flannigan, M.D., 2016. Future burn probability in south-central British Columbia. Int. J. Wildland Fire 25 (2), 200–212. https://doi.org/10.1071/WF15091.
Wang, X., Parisien, M.A., Taylor, S.W., Candau, J.N., Stralberg, D., Marshall, G.A., Little, J.M., Flannigan, M.D., 2017A. Projected changes in daily fire spread across Canada over the next century. Environ. Res. Lett. 12, 1–12. https://doi.org/10.1088/1748-9326/aa5835.
Wang, X., Wotton, B.M., Cantin, A.S., Parisien, M.-A., Anderson, K., Moore, B., Flannigan, M.D., 2017B. Cffdrs: an R package for the Canadian forest fire danger rating system. Ecol. Process. 6 (1), 5.
Wang, X., Studens, K., Parisien, M.A., Taylor, S.W., Candau, J.N., Boulanger, Y., Flannigan, M.D., 2020. Projected changes in fire size from daily spread potential in Canada over the 21st century. Environ. Res. Lett. 15, 104048.
Wang, X., Swystun, T., Oliver, J., Flannigan, M.D., 2021. One extreme fire weather event determines the extent and frequency of wildland fires. Environ. Res. Lett. https://doi.org/10.1088/1748-9326/ac2f64.
Wang, X., Swystun, T., Flannigan, M.D., 2022. Future wildfire extent and frequency determined by the longest fire-conducive weather spell. Sci. Total Environ. 154752.
Wood, S.N., 2011. Fast stable restricted maximum likelihood and marginal likelihood estimation of semiparametric generalized linear models. J. R. Stat. Soc. B 73 (1), 3–36.
Zong, X., Tian, X., Wang, X., 2021. An optimal firebreak design for the boreal forest of China. Sci. Total Environ. 781, 146822.